

Abstract

20

21 Surface incident solar radiation (R_s) plays a key role in climate change on Earth. R_s can
22 be directly measured, and it shows substantial variability on decadal scales, i.e., global
23 dimming and brightening. R_s can also be derived from the observed sunshine duration
24 (SunDu) with reliable accuracy. The SunDu-derived R_s has been used as a reference to
25 detect and adjust the inhomogeneity in the observed R_s . However, both the observed R_s
26 and SunDu-derived R_s may have inhomogeneity. In Japan, SunDu has been measured
27 since 1890, and R_s has been measured since 1961 at ~100 stations. In this study, the
28 observed R_s and SunDu-derived R_s were first checked for inhomogeneity independently
29 using a statistical software RHtest. If confirmed by the metadata of these observations,
30 the detected inhomogeneity was adjusted based on the RHtest-quantile matching
31 method. Second, the two homogenized time series were compared to detect further
32 possible inhomogeneity. If confirmed by the independent ground-based manual
33 observations of cloud cover fraction, the detected inhomogeneity was adjusted based
34 on the reference dataset. As a result, a sharp decrease of more than 20 W m^{-2} in the
35 observed R_s from 1961 to 1975 caused by instrument displacement was detected and
36 adjusted. Similarly, a decline of about 20 W m^{-2} in SunDu-derived R_s due to steady
37 instrument replacement from 1985 to 1990 was detected and adjusted too. After
38 homogenizations, the two estimates of R_s agree well. The homogenized SunDu-derived
39 R_s show an increased at a rate of 0.9 W m^{-2} per decade ($p < 0.01$) from 1961 to 2014,
40 which was caused by a positive aerosol-related radiative effect (2.2 W m^{-2} per decade)

41 and a negative cloud cover radiative effect (-1.4 W m^{-2} per decade). The brightening
42 over Japan was the strongest in spring, likely due to a significant decline in aerosol
43 transported from Asian dust storms. The observed raw R_s data and their homogenized
44 time series used in this study are available at
45 <https://doi.org/10.11888/Meteoro.tpsc.271524> (Ma et al., 2021).

46 **1. Introduction**

47 Surface incident solar radiation (R_s) plays a vital role in atmospheric circulation,
48 hydrologic cycling and ecological equilibrium; therefore, its decrease and increase
49 termed as global dimming and brightening (Wild et al., 2005; Shi et al., 2008), have
50 received widespread interest from the public and scientific community (Allen et al.,
51 2013; Xia, 2010; Wang et al., 2013; Tanaka et al., 2016; Ohmura, 2009; He et al., 2018).

52 In addition, the impact factors such as clouds and aerosols on the variation in R_s have
53 been widely studied (Wild et al., 2021; Qian et al., 2006; Feng and Wang, 2021a).

54 Ground-based observations of R_s are the first recommendation for detecting global
55 dimming and brightening. However, observational data may be inevitably ruined by
56 artificial shifts, which may lead to the variability in R_s with large uncertainties. Wang et
57 al. (2015) point out that instrument replacements and reconstruction of observational
58 network introduced substantial inhomogeneity into the time series of observed R_s over
59 China for 1990-1993. Manara et al. (2016) also show the instrument changes from the
60 Robitzsch pyranograph to the Kipp & Zonen CM11 pyranometer before 1980 caused
61 no clear dimming in Italy. Until recently, Wild et al. (2021) use a well-maintained data
62 series at a site in Germany with long time duration to investigate the dimming and
63 brightening in central Europe under clear sky condition, and point out that the aerosol
64 pollutants are likely major drivers in the R_s variations. Augustine and Hodges (2021)
65 use Surface Radiation Budget (SURFRAD) Network observations to explore the

66 variability in R_s over the U.S. from 1996 to 2019, and find that cloud fraction can
67 explain 62% of the variation of R_s , while aerosol optical depth (AOD) only accounts
68 for 3%. Both studies also indicate the measurement instruments have been changed
69 over the observational time periods, which may introduce non-climatic shifts and
70 inhomogeneity in the raw data series.

71 Homogenizing the observed R_s has been attempted in China (Wang et al., 2015;
72 Tang et al., 2011; Yang et al., 2018), Italy (Manara et al., 2016), Spain (Sanchez-
73 Lorenzo et al., 2013) and Europe (Sanchez-Lorenzo et al., 2015). It is essential to find
74 a homogeneous reference station to compare with the possible inhomogeneous station
75 to test and adjust the inhomogeneity in the observed time series, as done for the
76 homogenization of air temperature (Du et al., 2020; Zhou et al., 2021). However, this
77 process is difficult for R_s because the instrument replacement of R_s generally occurs
78 nearly simultaneously throughout a country. Therefore, the sunshine duration (SunDu)
79 derived R_s (Yang et al., 2006) has been used as a homogeneous reference dataset to
80 detect and adjust the inhomogeneity of R_s in China (Wang et al., 2015).

81 The SunDu records the hours of surface direct solar radiation exceeding 120 W m^{-2}
82 and provides an alternative way to estimate R_s (Yang et al., 2006; Stanhill and Cohen,
83 2008). SunDu-derived R_s is capable of capturing the variability in R_s . He et al. (2018)
84 use the SunDu-derived R_s at ~ 2600 stations to revisit the global dimming and
85 brightening over different continents, and restate the dimming over China and Europe
86 is consistent with the increasing trends of clouds and aerosols. Feng and Wang (2021b)

87 and Feng and Wang (2021a) merge the satellite retrievals with SunDu-derived R_s to
88 produce a high-resolution long-term solar radiation over China, and indicate cloud
89 fraction could explain approximately 86%–97% of R_s variation. Zeng et al. (2020)
90 demonstrate that SunDu plays a dominant role in determining R_s based on a random
91 forest model framework across China. Stanhill and Cohen (2005) indicate the high
92 correlation between SunDu and R_s at the 26 stations in the United States. Sanchez-
93 Lorenzo et al. (2008) show the variation in SunDu is consistent with that in R_s over
94 western Europe for 1938-2004, and the SunDu time evolution in Spring can partly be
95 explained by clouds and that in Winter can be related to the anthropogenic aerosol
96 emissions. Stanhill and Cohen (2008) establish a simple linear relationship between R_s
97 and SunDu to determine the long-term variation in R_s over Japan. Manara et al. (2017)
98 highlight that the atmospheric turbidity should be considered when using SunDu for
99 investigating multidecadal evolution of R_s .

100 Artificial shifts in SunDu observations may come from the replacement of
101 instruments. It has been revealed that the Jordan recorder is 10% more sensitive than
102 the Campbell-Stokes recorder for SunDu measurements (Noguchi, 1981). The
103 homogenization of SunDu has been carried out in Iberian Peninsula (Sanchez-Lorenzo
104 et al., 2007), Switzerland (Sanchez-Lorenzo and Wild, 2012), and Italy (Manara et al.,
105 2015).

106 The measurement of R_s , which started in 1961 in Japan, has a long history (Tanaka
107 et al., 2016), and a data record more than half a century-long has been accumulated.

108 The dataset has been widely used to study decadal variability (Wild et al., 2005; Stanhill
109 and Cohen, 2008) and to evaluate model simulations (Allen et al., 2013; Dwyer et al.,
110 2010). The Eppley and Robitzsch pyranometers used to measure R_s over Japan were
111 replaced by the Moll-Gorczyński thermopile pyranometers in the early 1970s (Tanaka
112 et al., 2016). However, the possible inhomogeneity of the observed R_s over Japan has
113 not been well quantified, and most existing studies directly used raw R_s data (Wild et
114 al., 2005; Tanaka et al., 2016; Tsutsumi and Murakami, 2012; Allen et al., 2013; Wild
115 and Schmucki, 2011; Kudo et al., 2012; Ohmura, 2009). Some studies have had to
116 abandon data from the early years and focused on only R_s data collected after 1975
117 (Tsutsumi and Murakami, 2012; Dwyer et al., 2010). Therefore, the observed decadal
118 variability in R_s over Japan is questionable, especially for the 1961-1975 time period.

119 In Japan, SunDu observations started in 1890, and more than a century-long data
120 were recorded. They cannot be too precious for the climate change detection on a
121 century scale. It is reported that the Jordan recorders used to measure SunDu were
122 replaced by EKO rotating mirror recorders in approximately 1986 (Inoue and
123 Matsumoto, 2003; Stanhill and Cohen, 2008). Therefore, SunDu observations over
124 Japan themselves may suffer inhomogeneity issues.

125 Non-climatic shifts in the observations may severely influence the climate
126 assessment, therefore rigorous homogenization is required. The world Meteorological
127 Organization (WMO) Climate Program guidelines on climate metadata and
128 homogenization list 14 data homogenization assessment techniques developed and

129 applied by different groups/authors (Aguilar et al., 2003). Reeves et al. (2007)
130 compared eight representative homogenization methods and provided guidelines for
131 which procedures work best in different situation, for example the standard normal
132 homogeneity (SNH) test (Alexandersson, 1986) works best if good reference series are
133 available and two-phase regressions of Wang procedure (Wang, 2003) is optimal for
134 good reference series unavailable condition. Based on the comparison work, RHtest
135 method was improved by detecting multiple changepoints in the climate data no matter
136 the reference series are available (Wang, 2008b; Wang et al., 2010; Wang et al., 2007;
137 Wang, 2008a). This method, which first detects the changepoints in a series using
138 penalized maximal tests and then tunes the inhomogeneous data segments to be
139 consistent with other segments in empirical distributions, has been widely used in
140 homogenizing climate variables (Dai et al., 2011; Wang et al., 2010; Du et al., 2020;
141 Zhou et al., 2021).

142 Discontinuities are inevitably occurred in the long-term observation system which
143 are required to be checked out and adjusted in the raw data. The homogenized series
144 pose a significant role in realistic and reliable assessment of climate trend and
145 variability. The main objective of this study is to detect and adjust the inhomogeneity
146 in R_s estimates over Japan. The metadata were first extracted from website information
147 and related records at each site. The SunDu observations were converted into R_s . The
148 RHtest method was applied to homogenize the observed R_s and SunDu-derived R_s , and
149 finally, the century-long homogenized R_s data were produced over Japan. Furthermore,

150 the impacts of cloud cover and aerosols on R_s variation over Japan in recent decades
151 were explored.

152 **2. Data and methods**

153 **2.1 Surface incident solar radiation and sunshine duration**

154 The monthly observed R_s at 105 stations and SunDu at 156 stations were
155 downloaded from the Japanese Meteorology Agency (JMA) website (see Table S1 and
156 Figure 1). R_s records were available from 1961. During the 1960s, two R_s measurements
157 were conducted in parallel by both Eppley and Robitzsch pyranometers. In the early
158 1970s (see Figure 2 and Table S2), these instruments were replaced by Moll-Gorczyński
159 thermopile pyranometers. This replacement occurred at approximately 12.4% of R_s
160 stations in 1971, followed by 22.9%, 24.8%, 3.8% and 30.5% in the next four years,
161 which may have caused severe data discontinuity problems (Tanaka et al., 2016).

162 SunDu has been routinely measured since 1890. Jordan recorders were replaced
163 by EKO rotating mirror recorders at 49.4% of SunDu stations in 1986. Until 1990,
164 nearly all of the SunDu stations used new instruments for observations. 4.5% of SunDu
165 stations before 1985 and 9.0% of SunDu stations after 2000 were moved away from the
166 original sites (see Figure 2 and Table S2) (Stanhill and Cohen, 2008).

167 In this study, SunDu was used to derive R_s based on the following equation (Yang
168 et al., 2006):

$$169 \quad R_s / R_c = a_0 + a_1 \cdot n/N + a_2 \cdot (n/N)^2 \quad (1)$$

170 where n is sunshine duration hours; N is the maximum possible sunshine duration; R_c
171 is surface solar radiation under clear skies; and a_0 , a_1 and a_2 are coefficients. This
172 method was recommended in many studies (Wang et al., 2015; Tang et al., 2011).

173 **2.2. Homogenization method**

174 Both R_s and SunDu measurements over Japan suffer severe inhomogeneity
175 problems, which require rigorous data homogenization. RHtest
176 (<http://etccdi.pacificclimate.org/software.shtml>) is a widely used method to detect and
177 adjust multiple changepoints in a climate data series, such as in surface temperature
178 (Du et al., 2020), radiosonde temperature (Zhou et al., 2021), precipitation (Wang et al.,
179 2010) and surface incident solar radiation (Yang et al., 2018) . Two algorithms were
180 provided to detect changepoints based on the penalized maximal T (PMT) test (Wang
181 et al., 2007) and the penalized maximal F (PMF) test (Wang, 2008b). The problem of
182 lag-1 autocorrelation in detecting mean shifts in time series was also resolved (Wang,
183 2008a). The PMT algorithm requires the base time series to be no trend, and hence a
184 reference series is needed. It is invalid when a reference series is not often available or
185 its homogeneity is not sure, also the trend in the base and reference series are probably
186 different. The PMF algorithm allows the time series in a constants trend and thus is
187 applicable without a reference series. Both algorithms have higher detection power and
188 the false alarm rate can be reduced by empirically constructed penalty function.

189 As the change of instrument in R_s and SunDu observation nearly happened
190 nationwide and simultaneously, it is difficult to find reference data series to match the

191 base data series and hence the PMF algorithm was used to detect the changepoints in
192 this study. Multiple changepoints were detected including climate signals and artificial
193 shifts, and only the ones confirmed by discontinuity information from metadata in Table
194 S2 were left to be adjusted. Then two homogenized series based on direct measurement
195 of R_s and SunDu-derived R_s were obtained.

196 Large uncertainties may still exist in both homogenized data series as the
197 discontinuities in the raw observations may not be sufficiently and correctly recorded
198 in the metadata. Further changepoints can be detected by considering the impact of the
199 variation of independent climate variables such as clouds and aerosols on the R_s
200 variation. If these uncertainties were found, further changepoint detections were needed
201 based on the PMT or PMF algorithm.

202 To diminish all significant artificial shifts caused by the changepoints, a newly
203 developed Quantile-Matching (QM) adjustments in the RHtest (Vincent et al., 2012;
204 Wang et al., 2010) were performed to adjust the series so that the empirical distributions
205 of all segments of the detrended base series agree with each other. The corrected values
206 are all based on the empirical frequency of the datum to be adjusted.

207 Another independent homogenization method proposed by Katsuyama (1987),
208 which was developed due to the replacement of the Jordan recorders with EKO rotating
209 mirror recorder during the late 1980s, is denoted as follows:

$$210 \quad S_R = 0.8 S_J (S_J < 2.5 \text{ h/day}) \quad (2)$$

$$211 \quad S_R = S_J - 0.5 \text{ h/day} (S_J \geq 2.5 \text{ h/day}) \quad (3)$$

212 where S_J is the daily SunDu observed by the Jordan recorders before replacement; and
213 S_R is the daily SunDu adjusted to be consistent with the values observed with the EKO
214 rotating mirror recorders.

215 These two homogenization methods were compared in this study and yielded
216 nearly the same SunDu-derived R_s variation, as shown in Figure 3. Although the
217 second method proposed by Katsuyama (1987) is simple and efficient, we just use it
218 to cross validate the accuracy of the RHtest method. For the following analysis, the
219 SunDu-derived R_s homogenized by RHtest was used as RHtest method provides
220 higher power to detect the changepoints in a data series no matter the metadata are
221 available. Since most artificial shifts in observation system were undocumented
222 worldwide, the statistical methods including RHtest are optimal to identify these non-
223 climatic signals and reduce the discontinuities in the data series.

224 **2.3 Clouds**

225 Clouds play an important role in R_s variation (Norris and Wild, 2009). Monthly
226 cloud cover observations at 155 stations were also available on the JMA website. The
227 observation time for cloud amount has been 08:00-19:00 since 1981 at 9.0% of cloud
228 amount stations and 08:30-17:00 from 1990 to 1995 at another 15.4% of cloud amount
229 stations (see Figure 2 and Table S2). However, the difference between annual raw and
230 homogenized cloud data is trivial, as cloud data are relatively homogeneous in space
231 compared with R_s and SunDu observations. A site observation of cloud amount can
232 represent the value over a large spatial scale, likely leading to few inhomogeneity issues

233 for cloud data.

234 To explore the impact of the cloud cover anomaly on the R_s variation, the cloud
235 cover radiative effect (CCRE), defined as the change in R_s produced by a change in
236 cloud cover, was proposed by (Norris and Wild, 2009):

$$237 \quad CCRE' (lat, lon, y, m) = CC' (lat, lon, y, m) \times CRE(g, m) / \overline{CC}(g, m) \quad (4)$$

238 where lat is the latitude, lon is the longitude, y is the year, m is the month, $CCRE'$
239 is the cloud cover radiative effect anomaly, CC' is the cloud cover anomaly, \overline{CC} is
240 the climatology of cloud cover in 12 months and CRE is the cloud radiative effect
241 calculated by the R_s difference under all sky and clear sky conditions.

242 The residual radiative effect was determined by removing the CCRE anomalies
243 from the R_s anomalies. It is noted that a part of the cloud albedo radiative effect
244 proportional to the cloud amount was contained in the CCRE, as a large cloud amount
245 tends to yield enhanced cloud albedo, whereas another part of the cloud albedo radiative
246 effect due to the aerosol first indirect effect (more aerosols facilitating more cloud
247 condensation nuclei may enhance cloud albedo) may be included in the residual
248 radiative effect, which mainly contains the aerosol radiative effect.

249 The Clouds and the Earth's Radiant Energy System (CERES) provides a reliable
250 surface incident solar radiation (Ma et al., 2015) primarily based on the Moderate
251 Resolution Imaging Spectroradiometer (MODIS) cloud and aerosol products (Kato et
252 al., 2012). The cloud amount in CERES agrees well with the observations, and the
253 annual CRE in CERES is well correlated with the annual cloud amount in Figure 10.

254 The regional average cloud amount over Japan in Figure 10 (blue line) increases at a
255 rate of 0.7% per decade from 1960 to 2015, which is consistent with the previous results
256 (Figure 4 in Tsutsumi and Murakami (2012)).

257 In this study, long-term observations of cloud amount and monthly cloud radiative
258 effect (CRE) data in the CERES EBAF edition were used following Equation (4) to
259 distinguish the cloud cover radiative effect from R_s variation.

260 **2.4 Data Processing**

261 We first interpolated the monthly observational data at sites into $1^\circ \times 1^\circ$ grid data,
262 and then calculated the area average of the climate variables. As the brightening and
263 dimming over Japan were the main concern in this study, monthly values were
264 converted into annual values for calculation. If there are missing values in any month
265 in a specific year, the annual value for that year is set to a missing value. The linear
266 regression was used for trend calculation.

267 **3. Results**

268 In this section, we first compared the observed R_s and sunshine duration derived
269 R_s before and after adjustment to demonstrate the necessity and feasibility of the
270 homogenization procedure in Section 3.1. As artificial shifts may not be sufficiently
271 and correctly documented by metadata, uncertainties may still exist in the homogenized
272 series. We then tried to explore these uncertainties by considering the influence of other
273 independent climate variables such as clouds, aerosols on the R_s variation, and

274 ultimately informed a more reasonable homogenized R_s series in Section 3.2. In Section
275 3.3, we claimed the significant correction in trend analysis of R_s in Japan and quantified
276 the influence of clouds and aerosols on the R_s variation.

277 **3.1 Homogenization of observed R_s and sunshine duration derived R_s**

278 The comparisons between raw data and homogenized data at each site were
279 shown in Figure 4 and their difference were illustrated in Figure 5. Compared with
280 raw data, the absolute values of biases between R_s and SunDu-derived R_s at 74 stations
281 decrease after homogenization, of which the absolute values of biases decrease by
282 more than 4 W m^{-2} at 42 stations and more than 10 W m^{-2} at 8 stations. The root mean
283 square errors at 80 stations were reduced after homogenization, of which reduces are
284 more than 4 W m^{-2} at 40 stations. After adjustments, the correlation coefficients
285 between the annual observed R_s and annual SunDu-derived R_s are improved at 68
286 stations, including greater than 0.2 improvement at 31 stations. There are 41 stations
287 (marked with red in Table S1, Figure 6) at which the correlation coefficients were
288 greater than 0.5, and the biases and the root mean square errors generally decrease
289 after homogenization.

290 Figure 7, as an example, shows the time series of surface incident solar radiation
291 (R_s and SunDu-derived R_s) at the HAMADA site (WMO-ID: 47755, Lat: 34.9, Lon:
292 132.07) before and after homogenization. Details in the improvements after
293 homogenization at most stations can be traced back to Figures 4, 5 and 6. The
294 improved patterns of time series of surface incident solar radiation after

295 homogenization highlights the necessity and feasibility of the RHtest method. The
296 SunDu-derived R_s variation over Japan during recent decades inferred from these
297 “perfect” data at 41 sites (Figure 8) was nearly identical to that from all available data
298 at 156 sites (as shown in Table 1 and Figure 9).

299 **3.2 Uncertainties in R_s observations**

300 Figure 9 displays the change in R_s during the last 5 decades, while Figure 10 shows
301 the variation in observed clouds over Japan. The sharp decrease in R_s in 1963 caused
302 by the volcanic eruption of Agung in Indonesia (Witham, 2005) can be clearly found.
303 The sharp decreases in R_s in 1991 and 1993 are due to the combined effect of the
304 volcanic eruption of Mount Pinatubo in the Philippines in 1991 (Robock, 2000) and the
305 simultaneous significant increases in clouds (Figure 8 in Tsutsumi and Murakami
306 (2012)). The volcanic eruption of El Chichón in Mexico in 1982 exerted little impact
307 on the decline in R_s and may have been compensated by the decrease in clouds, as shown
308 in Figure 10. The pronounced R_s decline in 1980 coincides with the significant increase
309 in clouds, while the lightening of R_s in 1978 and 1994 encounters abrupt decreases in
310 cloud covers.

311 As shown in Figure 9, no major modifications were found in R_s observations
312 before and after homogenization (comparison between the light blue and dark blue
313 lines). However, the SunDu-derived R_s series are smoother after adjustment by the QM
314 method, as the sharp decrease from 1983 to 1993 caused by the replacement of sunshine
315 duration instruments (Jordan recorders were replaced with EKO rotating mirror

316 recorders) (Stanhill and Cohen, 2008) was repaired (comparison between the light red
317 line and dark red lines). Despite the identical increase in R_s via both the homogenized
318 direct measurements of R_s and the homogenized SunDu-derived R_s during the 1995-
319 2014 period, their variations in R_s from 1961 to 1994 are different (dark red line and
320 dark blue line).

321 Large discrepancies in R_s variation were found during the time period of 1961-
322 1970, although homogenizations were performed on the direct measurements of R_s and
323 SunDu-derived R_s (dark blue line and dark red line in Figure 9). Existing study noted
324 the inaccurate instruments used at the beginning of operation in the R_s observation
325 network in approximately 1961, and the parallel use of two different types of
326 instruments during the 1960s may result in the large variability in observed R_s (Tanaka
327 et al., 2016). At this time, the clouds fluctuated gently, as shown in Figure 10, and the
328 change in volcanic aerosols from 1965 to 1966 was nearly the same as that from 1962
329 to 1963 (Table 2 in Sato et al. (1993)), so the sudden decline in the direct observations
330 of R_s from 1965 to 1966, which was twice as large as that from 1962 to 1963, is
331 suspicious. It is inferred that anthropogenic aerosols play a subtle role in the significant
332 reduction in R_s , as this type of phenomenon is common for both polluted and pristine
333 stations in Japan (Figure 22 in (Tanaka et al., 2016)).

334 Figure 11 shows the correlation coefficients between homogenized R_s (observed
335 and SunDu-derived) and cloud amount. In general, the observed R_s (-0.45) is less
336 correlated than the SunDu-derived R_s (-0.67), particularly from 1961 to 1970, -0.21

337 compared with -0.64. This in turn supports the reliability of homogenized SunDu-
338 derived R_s , especially during the time period of 1961-1970. The false variability of the
339 observed R_s from 1961 to 1970 was modified by the RHtest method against the
340 homogenized SunDu-derived R_s as shown in Figure 12.

341 General decreases in stratospheric aerosol optical depth (AOD) were reported in
342 Sato et al. (1993) from 1965 to 1980, and clouds fluctuated slightly, as shown in Figure
343 10; both of these factors contributed to a brightening of R_s . This agrees with the SunDu-
344 derived R_s and contrasts with the direct measurements of R_s .

345 During the 1985-1990 period, clouds varied slightly, as shown in Figure 10, and
346 the observed atmospheric transmission under cloud-free conditions increased (Wild et
347 al., 2005), which suggests that the large declines in directly observed R_s and SunDu-
348 derived R_s are defective and reinforce the reliability of the adjusted SunDu-derived R_s
349 (dark red line in Figure 9).

350 From the above analysis, it can be inferred that fewer uncertainties exist in
351 homogenized SunDu-derived R_s , which was confirmed by another work that utilized a
352 different data adjusted method (Stanhill and Cohen, 2008). However, quantifying the
353 accuracy of homogenized SunDu-derived R_s seems not to be accessible until more
354 accurate observations of R_s are available.

355 **3.2 Trends of R_s over Japan**

356 The trends of R_s during specific time periods for different types of datasets are
357 listed in Table 1. Direct measurements of R_s and SunDu-derived R_s from 41 selected
358 stations and all available stations reveal similar variations in R_s over Japan, which

359 demonstrates that the sample number has a subtle impact on the estimation of global
360 brightening and dimming over Japan.

361 A revisit of global dimming and brightening was list in Table 1. Major differences
362 were found in the time periods of 1961-1980, ranging from -11.2 (-12.0) to -8.4 (-4.8)
363 W m^{-2} per decade before and after R_s homogenizations for all available stations (41
364 selected stations) over Japan; significant repairs occurred during the 1981-1995 period,
365 ranging from -10.6 (-11.3) to -1.2 (-1.3) W m^{-2} per decade before and after SunDu-
366 derived R_s homogenizations for all available stations (41 selected stations) over Japan.
367 Both corrections were mainly attributed to the homogenization of corrupted raw data
368 caused by the replacement of instruments for R_s and SunDu measurements. After
369 careful checking and adjustment of the SunDu-derived R_s series, the decadal variation
370 in R_s over Japan, which was totally different from former studies (Wild et al., 2005;
371 Norris and Wild, 2009), was remedied. Direct measurements of R_s display nearly zero
372 trend from 1961 to 2014 over Japan, while their homogenization series report a positive
373 change of 0.8-1.6 W m^{-2} per decade; SunDu-derived R_s decrease at a rate of 1.9 W m^{-2}
374 per decade, while its homogenized series reveals a brightening of 0.9 W m^{-2} per decade.

375 The combined effects of clouds and aerosols on R_s make the global dimming and
376 brightening complicated. The CCRE can explain 70% of global brightening from 1961
377 to 2014 at monthly and interannual time scales, while the residual radiative effect
378 dominates the decadal variation in R_s , as shown in Figure 13 and Table 1, which is in
379 agreement with Wang et al. (2012). Homogenized SunDu-derived R_s show an increase

380 of 1.6 W m^{-2} per decade from 1961 to 1980; however, persistent increase in cloud
381 amount yields a CCRE decrease of 1.1 W m^{-2} per decade. The residual radiative effect
382 accounts for an increase of 2.4 W m^{-2} per decade for this time period. The cloud
383 radiative effect (-1.4 W m^{-2} per decade) modulates R_s variation of -1.2 W m^{-2} per decade
384 for the 1981-1995 period, while the residual radiative effect (1.2 W m^{-2} per decade)
385 dominates R_s variation of 1.4 W m^{-2} per decade from 1996 to 2014.

386 Homogenized SunDu-derived R_s shows a slight increase of 0.9 W m^{-2} per decade
387 from 1961 to 2014 with a 90% confidence interval. However, the CCRE accounts for a
388 decreased R_s of 1.4 W m^{-2} per decade, which implies that cloud cover changes are not
389 the primary driving forces for the R_s trend over Japan. Meanwhile, the residual radiative
390 effect exhibits an increase of 2.2 W m^{-2} per decade, which surpasses the negative CCRE.

391 Several studies demonstrate a generally cleaner sky over Japan from the 1960s to
392 the 2000s (except for the years impacted by volcanic eruptions) based on atmospheric
393 transparency and aerosol optical properties (Wild et al., 2005; Kudo et al., 2012), which
394 supports the dominant role of aerosols in R_s brightening over Japan, as revealed by the
395 residual radiative effect here. Furthermore, the residual radiative effect in this study is
396 stronger than that in Norris and Wild (2009), as raw data were remedied and more
397 accurate satellite data from CERES were adopted to quantify the radiative effect.
398 Tsutsumi and Murakami (2012) demonstrate that cloud amount categories exert an
399 important effect on R_s variation. R_s enhancement by the increased appearance of large
400 cloud amounts is superior to R_s decline by the decreased appearance of small cloud

401 amounts during 1961-2014, which yields increased R_s with increasing total cloud
402 amount. They also pointed out that the decrease in cloud optical thickness due to the
403 large emissions of SO_2 and black carbon from East Asia through the aerosol semi-direct
404 effect (absorption of more energy by aerosols results in the evaporation or suppression
405 of clouds) may have facilitated the increased R_s over Japan.

406 The decrease in spring dust storms in March-May during the last 5 decades from
407 China (Qian et al., 2002; Zhu et al., 2008), which may travel to neighboring
408 countries(Uno et al., 2008; Choi et al., 2001), could also have triggered the increase in
409 R_s over Japan. The R_s variation and radiative effect in different seasons are categorized
410 in Figure 14 and Table 2, in which an increasing trend of 1.5 W m^{-2} per decade in the
411 homogenized SunDu-derived R_s prevails in spring for the whole time period, dominated
412 by a dramatic increase of 2.8 W m^{-2} per decade in the residual effect and even larger
413 increase for 1961-1980 (3.1 W m^{-2} per decade) and 1996-2014 (3.4 W m^{-2} per decade).

414 **4. Data availability**

415 Monthly observed surface incident solar radiation, sunshine duration and cloud
416 amount data were provided by Japan Meteorological Agency
417 (<https://www.data.jma.go.jp/obd/stats/data/en/smp/index.html>), and monthly cloud
418 radiative effect (CRE) data were derived from Clouds and the Earth's Radiant Energy
419 System for CERES EBAF data (https://ceres.larc.nasa.gov/order_data.php). The
420 homogenized observed R_s and SunDu-derived R_s used in this study are available at

421 [https://doi.org/10.11888/Meteoro.tpsc.271524_\(Ma et al., 2021\)](https://doi.org/10.11888/Meteoro.tpsc.271524_(Ma et al., 2021)).

422 **5. Conclusions**

423 The homogenization of raw observations related to R_s can significantly improve
424 the accuracy of global dimming and brightening estimation and provide a reliable
425 assessment of climate trends and variability. In this study, we for the first time
426 homogenized the raw R_s observations and obtained a more reliable R_s data series over
427 Japan for century-long.

428 Documented artificial shifts in metadata play an important role in regulating the
429 raw observations. If changepoints were confirmed by metadata or other independent
430 climate variables, RHtest method was applied to remove the discontinuities. In this
431 study, shifts in the homogenized raw R_s were further checked by exploring the
432 relationship with the ground-based cloud amount and tuned again using homogenized
433 SunDu-derived R_s as the reference data. By comparing the variations in independent
434 climate variables of cloud and aerosol, the homogenized SunDu-derived R_s were proved
435 to be more reliable in detecting R_s variability over Japan.

436 A revisit of global dimming and brightening is made based on the homogenized
437 R_s series. R_s over Japan increases at a rate of 1.6 W m^{-2} per decade for 1961-1980, which
438 is contrary to the trend ($-4.8 \sim -12.0 \text{ W m}^{-2}$ per decade) in the unreasonable R_s
439 observation. A slight decrease of 1.2 W m^{-2} per decade for 1981-1995 in homogenized
440 SunDu-derived R_s accounts for only 1/10 of the trend in its unadjusted series. This

441 directly contributes a brightening of 0.9 W m^{-2} per decade (with a 99% confidence
442 interval) for the last 5 decades in homogenized series, which is totally contrary to the
443 variation in its original series. Global brightening since 1961 over Japan is consistent
444 with that in Stanhill and Cohen (2008), except that the magnitude is not as large.

445 We also explored how the clouds and aerosols mediate the transformation of R_s .
446 The brightening in Japan for 1961-1980 was the combined effect of cloud cover
447 (negative effect) and aerosols (positive effect). The dimming for 1981-1995 was
448 governed by reduced cloud amounts, while the increase in R_s for 1996-2014 was
449 controlled by decreased aerosols. These results are different from those in Norris and
450 Wild (2009), as homogenization was performed on the raw data and more accurate
451 cloud radiative effect data series from CERES were utilized in our study. During the
452 entire period of 1961-2014, cloud amounts dominated seasonal and interannual R_s
453 variations, while aerosols (including aerosol-cloud interactions) drove decadal R_s
454 variations over Japan, noted by other studies, in response to general cleaner skies and a
455 reduction in spring Asian dust storms (Wang et al., 2012; Kudo et al., 2012).

456

457 **Author contributions**

458 QM and KW designed the research and wrote the paper. LS collected the raw data. YH
459 homogenized the raw data. QW provided the technical support. YZ and HL checked the
460 data.

461

462 **Competing interests**

463 The authors declare that they have no conflict of interest.

464

465

466

467

Acknowledgements

468 This study is funded by the National Key R&D Program of China (2017YFA0603601),

469 the National Science Foundation of China (41930970), and Project Supported by State

470 Key Laboratory of Earth Surface Processes and Resource Ecology (2017-KF-03). We

471 thank many institutions for sharing their data: Japan Meteorological Agency for

472 observation data over Japan

473 (<https://www.data.jma.go.jp/obd/stats/data/en/smp/index.html>); Clouds and the Earth's

474 Radiant Energy System for CERES EBAF data

475 (https://ceres.larc.nasa.gov/order_data.php). We thank the Expert Team on Climate

476 Change Detection and Indices (ETCCDI) for providing the RHtestV4 homogenization

477 package (<http://etccdi.pacificclimate.org/software.shtml>).

478

479

481 **References**

- 482 Aguilar, E., Auer, I., Brunet, M., Peterson, T. C., and Wieringa, J.: Guidelines on
483 climate metadata and homogenization, WMO-TD No. 1186, 1186, 2003.
- 484 Alexandersson, H.: A homogeneity test applied to precipitation data, 6, 661-675,
485 <https://doi.org/10.1002/joc.3370060607>, 1986.
- 486 Allen, R. J., Norris, J. R., and Wild, M.: Evaluation of multidecadal variability in
487 CMIP5 surface solar radiation and inferred underestimation of aerosol direct effects
488 over Europe, China, Japan, and India, *J Geophys Res-Atmos*, 118, 6311-6336,
489 10.1002/jgrd.50426, 2013.
- 490 Augustine, J. A. and Hodges, G. B.: Variability of Surface Radiation Budget
491 Components Over the U.S. From 1996 to 2019—Has Brightening Ceased?, 126,
492 e2020JD033590, <https://doi.org/10.1029/2020JD033590>, 2021.
- 493 Choi, J. C., Lee, M., Chun, Y., Kim, J., and Oh, S.: Chemical composition and source
494 signature of spring aerosol in Seoul, Korea, *J Geophys Res-Atmos*, 106, 18067-
495 18074, <https://doi.org/10.1029/2001JD900090>, 2001.
- 496 Dai, A., Wang, J., Thorne, P. W., Parker, D. E., Haimberger, L., and Wang, X. L.: A
497 New Approach to Homogenize Daily Radiosonde Humidity Data, *J Climate*, 24, 965-
498 991, 10.1175/2010jcli3816.1, 2011.
- 499 Du, J., Wang, K., Cui, B., and Jiang, S.: Correction of Inhomogeneities in Observed
500 Land Surface Temperatures over China, *J Climate*, 33, 8885-8902, 10.1175/jcli-d-19-
501 0521.1, 2020.
- 502 Dwyer, J. G., Norris, J. R., and Ruckstuhl, C.: Do climate models reproduce observed
503 solar dimming and brightening over China and Japan?, *J Geophys Res-Atmos*, 115,
504 <https://doi.org/10.1029/2009JD012945>, 2010.
- 505 Feng, F. and Wang, K.: Merging ground-based sunshine duration observations with
506 satellite cloud and aerosol retrievals to produce high-resolution long-term surface
507 solar radiation over China, *Earth Syst. Sci. Data*, 13, 907-922, 10.5194/essd-13-907-
508 2021, 2021a.
- 509 Feng, F. and Wang, K.: Merging High-Resolution Satellite Surface Radiation Data
510 with Meteorological Sunshine Duration Observations over China from 1983 to 2017,
511 *Remote Sens*, 13, 602, <https://doi.org/10.3390/rs13040602>, 2021b.
- 512 He, Y., Wang, K., Zhou, C., and Wild, M.: A Revisit of Global Dimming and
513 Brightening Based on the Sunshine Duration, 45, 4281-4289,
514 <https://doi.org/10.1029/2018GL077424>, 2018.
- 515 Inoue, T. and Matsumoto, J.: Seasonal and secular variations of sunshine duration and
516 natural seasons in Japan, *Int J Climatol*, 23, 1219-1234, 10.1002/joc.933, 2003.
- 517 Kato, S., Loeb, N. G., Rose, F. G., Doelling, D. R., Rutan, D. A., Caldwell, T. E., Yu,
518 L., and Weller, R. A.: Surface Irradiances Consistent with CERES-Derived Top-of-

519 Atmosphere Shortwave and Longwave Irradiances, *J Climate*, 26, 2719-2740,
520 10.1175/jcli-d-12-00436.1, 2012.

521 Katsuyama, M.: On comparison between rotating mirror sunshine recorders and
522 Jordan sunshine recorders, *Weather Service Bulletin*, 54, 169-183, 1987.

523 Kudo, R., Uchiyama, A., Ijima, O., Ohkawara, N., and Ohta, S.: Aerosol impact on the
524 brightening in Japan, *J Geophys Res-Atmos*, 117,
525 <https://doi.org/10.1029/2011JD017158>, 2012.

526 Ma, Q., Wang, K. C., and Wild, M.: Impact of geolocations of validation data on the
527 evaluation of surface incident shortwave radiation from Earth System Models, *J*
528 *Geophys Res-Atmos*, 120, 6825-6844, 10.1002/2014JD022572, 2015.

529 Ma, Q., He, Y., Wang, K., and Su, L.: Homogenized solar radiation data set over
530 Japan (1870-2015), National Tibetan Plateau Data Center [dataset],
531 10.11888/Meteoro.tpdc.271524, 2021.

532 Manara, V., Brunetti, M., Maugeri, M., Sanchez-Lorenzo, A., and Wild, M.: Sunshine
533 duration and global radiation trends in Italy (1959–2013): To what extent do they
534 agree?, 122, 4312-4331, <https://doi.org/10.1002/2016JD026374>, 2017.

535 Manara, V., Brunetti, M., Celozzi, A., Maugeri, M., Sanchez-Lorenzo, A., and Wild,
536 M.: Detection of dimming/brightening in Italy from homogenized all-sky and clear-
537 sky surface solar radiation records and underlying causes (1959–2013), *Atmos Chem*
538 *Phys*, 16, 11145-11161, 10.5194/acp-16-11145-2016, 2016.

539 Manara, V., Beltrano, M. C., Brunetti, M., Maugeri, M., Sanchez-Lorenzo, A.,
540 Simolo, C., and Sorrenti, S.: Sunshine duration variability and trends in Italy from
541 homogenized instrumental time series (1936–2013), *J Geophys Res-Atmos*, 120,
542 3622-3641, <https://doi.org/10.1002/2014JD022560>, 2015.

543 Noguchi, Y.: Solar radiation and sunshine duration in East Asia, *Archives for*
544 *meteorology, geophysics, and bioclimatology, Series B*, 29, 111-128,
545 10.1007/BF02278195, 1981.

546 Norris, J. R. and Wild, M.: Trends in aerosol radiative effects over China and Japan
547 inferred from observed cloud cover, solar “dimming,” and solar “brightening”, *J*
548 *Geophys Res-Atmos*, 114, <https://doi.org/10.1029/2008JD011378>, 2009.

549 Ohmura, A.: Observed decadal variations in surface solar radiation and their causes, *J*
550 *Geophys Res-Atmos*, 114, <https://doi.org/10.1029/2008JD011290>, 2009.

551 Qian, W., Quan, L., and Shi, S.: Variations of the Dust Storm in China and its Climatic
552 Control, *J Climate*, 15, 1216-1229, 10.1175/1520-
553 0442(2002)015<1216:Votdsi>2.0.Co;2, 2002.

554 Qian, Y., Kaiser, D. P., Leung, L. R., and Xu, M.: More frequent cloud-free sky and
555 less surface solar radiation in China from 1955 to 2000, *Geophys Res Lett*, 33, Artn
556 L01812
557 Doi 10.1029/2005gl024586, 2006.

558 Reeves, J., Chen, J., Wang, X. L., Lund, R., and Lu, Q. Q.: A Review and Comparison
559 of Change-point Detection Techniques for Climate Data %J *Journal of Applied*

560 Meteorology and Climatology, 46, 900-915, 10.1175/jam2493.1, 2007.

561 Robock, A.: Volcanic eruptions and climate, *Rev Geophys*, 38, 191-219,

562 <https://doi.org/10.1029/1998RG000054>, 2000.

563 Sanchez-Lorenzo, A. and Wild, M.: Decadal variations in estimated surface solar

564 radiation over Switzerland since the late 19th century, *Atmos Chem Phys*, 12, 8635-

565 8644, 10.5194/acp-12-8635-2012, 2012.

566 Sanchez-Lorenzo, A., Calbó, J., and Martin-Vide, J.: Spatial and Temporal Trends in

567 Sunshine Duration over Western Europe (1938–2004), *J Climate*, 21, 6089-6098,

568 10.1175/2008jcli2442.1, 2008.

569 Sanchez-Lorenzo, A., Calbó, J., and Wild, M.: Global and diffuse solar radiation in

570 Spain: Building a homogeneous dataset and assessing their trends, *Global Planet*

571 *Change*, 100, 343-352, <https://doi.org/10.1016/j.gloplacha.2012.11.010>, 2013.

572 Sanchez-Lorenzo, A., Brunetti, M., Calbó, J., and Martin-Vide, J.: Recent spatial and

573 temporal variability and trends of sunshine duration over the Iberian Peninsula from a

574 homogenized data set, *J Geophys Res-Atmos*, 112,

575 <https://doi.org/10.1029/2007JD008677>, 2007.

576 Sanchez-Lorenzo, A., Wild, M., Brunetti, M., Guijarro, J. A., Hakuba, M. Z., Calbó,

577 J., Mystakidis, S., and Bartok, B.: Reassessment and update of long-term trends in

578 downward surface shortwave radiation over Europe (1939–2012), *J Geophys Res-*

579 *Atmos*, 120, 9555-9569, <https://doi.org/10.1002/2015JD023321>, 2015.

580 Sato, M., Hansen, J. E., McCormick, M. P., and Pollack, J. B.: Stratospheric aerosol

581 optical depths, 1850–1990, *J Geophys Res-Atmos*, 98, 22987-22994,

582 <https://doi.org/10.1029/93JD02553>, 1993.

583 Shi, G. Y., Hayasaka, T., Ohmura, A., Chen, Z. H., Wang, B., Zhao, J. Q., Che, H. Z.,

584 and Xu, L.: Data quality assessment and the long-term trend of ground solar radiation

585 in China, *J Appl Meteorol Clim*, 47, 1006-1016, Doi 10.1175/2007jamc1493.1, 2008.

586 Stanhill, G. and Cohen, S.: Solar Radiation Changes in the United States during the

587 Twentieth Century: Evidence from Sunshine Duration Measurements, *J Climate*, 18,

588 1503-1512, 10.1175/jcli3354.1, 2005.

589 Stanhill, G. and Cohen, S.: Solar Radiation Changes in Japan during the 20th Century:

590 Evidence from Sunshine Duration Measurements, *J Meteorol Soc Jpn. Ser. II*, 86, 57-

591 67, 10.2151/jmsj.86.57, 2008.

592 Tanaka, K., Ohmura, A., Folini, D., Wild, M., and Ohkawara, N.: Is global dimming

593 and brightening in Japan limited to urban areas?, *Atmospheric Chemistry And*

594 *Physics*, 16, 13969-14001, 10.5194/acp-16-13969-2016, 2016.

595 Tang, W. J., Yang, K., Qin, J., Cheng, C. C. K., and He, J.: Solar radiation trend across

596 China in recent decades: a revisit with quality-controlled data, *Atmos Chem Phys*, 11,

597 393-406, 10.5194/acp-11-393-2011, 2011.

598 Tsutsumi, Y. and Murakami, S.: Increase in Global Solar Radiation with Total Cloud

599 Amount from 33 Years Observations in Japan, *J Meteorol Soc Jpn*, 90, 575-581,

600 10.2151/jmsj.2012-409, 2012.

601 Uno, I., Yumimoto, K., Shimizu, A., Hara, Y., Sugimoto, N., Wang, Z., Liu, Z., and
602 Winker, D. M.: 3D structure of Asian dust transport revealed by CALIPSO lidar and a
603 4DVAR dust model, *Geophys Res Lett*, 35, <https://doi.org/10.1029/2007GL032329>,
604 2008.

605 Vincent, L. A., Wang, X. L., Milewska, E. J., Wan, H., Yang, F., and Swail, V.: A
606 second generation of homogenized Canadian monthly surface air temperature for
607 climate trend analysis, *J Geophys Res-Atmos*, 117,
608 <https://doi.org/10.1029/2012JD017859>, 2012.

609 Wang, K. C., Dickinson, R. E., Wild, M., and Liang, S.: Atmospheric impacts on
610 climatic variability of surface incident solar radiation, *Atmos Chem Phys*, 12, 9581-
611 9592, 10.5194/acp-12-9581-2012, 2012.

612 Wang, K. C., Ma, Q., Li, Z. J., and Wang, J. K.: Decadal variability of surface incident
613 solar radiation over China: Observations, satellite retrievals, and reanalyses, *J*
614 *Geophys Res-Atmos*, 120, 6500-6514, 10.1002/2015JD023420, 2015.

615 Wang, K. C., Dickinson, R. E., Ma, Q., Augustine, J. A., and Wild, M.: Measurement
616 Methods Affect the Observed Global Dimming and Brightening, *J Climate*, 26, 4112-
617 4120, 10.1175/Jcli-D-12-00482.1, 2013.

618 Wang, X. L.: Comments on “Detection of Undocumented Changepoints: A Revision
619 of the Two-Phase Regression Model” %J *Journal of Climate*, 16, 3383-3385,
620 10.1175/1520-0442(2003)016<3383:Codouc>2.0.Co;2, 2003.

621 Wang, X. L.: Accounting for Autocorrelation in Detecting Mean Shifts in Climate
622 Data Series Using the Penalized Maximal t or F Test, *J Appl Meteorol Clim*, 47, 2423-
623 2444, 10.1175/2008jamc1741.1, 2008a.

624 Wang, X. L., Wen, Q. H., and Wu, Y.: Penalized Maximal t Test for Detecting
625 Undocumented Mean Change in Climate Data Series, *J Appl Meteorol Clim*, 46, 916-
626 931, 10.1175/jam2504.1, 2007.

627 Wang, X. L. L.: Penalized maximal F test for detecting undocumented mean shift
628 without trend change, *J Atmos Ocean Technol*, 25, 368-384,
629 10.1175/2007JTECHA982.1, 2008b.

630 Wang, X. L. L., Chen, H. F., Wu, Y. H., Feng, Y., and Pu, Q. A.: New Techniques for
631 the Detection and Adjustment of Shifts in Daily Precipitation Data Series, *J Appl*
632 *Meteorol Clim*, 49, 2416-2436, 10.1175/2010JAMC2376.1, 2010.

633 Wild, M. and Schmucki, E.: Assessment of global dimming and brightening in IPCC-
634 AR4/CMIP3 models and ERA40, *Clim Dynam*, 37, 1671-1688, 10.1007/s00382-010-
635 0939-3, 2011.

636 Wild, M., Wacker, S., Yang, S., and Sanchez-Lorenzo, A.: Evidence for Clear-Sky
637 Dimming and Brightening in Central Europe, 48, e2020GL092216,
638 <https://doi.org/10.1029/2020GL092216>, 2021.

639 Wild, M., Gilgen, H., Roesch, A., Ohmura, A., Long, C. N., Dutton, E. G., Forgan, B.,
640 Kallis, A., Russak, V., and Tsvetkov, A.: From Dimming to Brightening: Decadal
641 Changes in Solar Radiation at Earth's Surface, *Science*, 308, 847-850,

642 10.1126/science.1103215, 2005.
643 Witham, C. S.: Volcanic disasters and incidents: A new database, *J Volcanol Geoth*
644 *Res*, 148, 191-233, 10.1016/j.jvolgeores.2005.04.017, 2005.
645 Xia, X.: A closer looking at dimming and brightening in China during 1961-2005,
646 *Ann Geophys*, 28, 1121-1132, 10.5194/angeo-28-1121-2010, 2010.
647 Yang, K., Koike, T., and Ye, B. S.: Improving estimation of hourly, daily, and monthly
648 solar radiation by importing global data sets, *Agr Forest Meteorol*, 137, 43-55,
649 10.1016/j.agrformet.2006.02.001, 2006.
650 Yang, S., Wang, X. L., and Wild, M.: Homogenization and Trend Analysis of the
651 1958–2016 In Situ Surface Solar Radiation Records in China, *J Clim*, 31, 4529-4541,
652 10.1175/jcli-d-17-0891.1, 2018.
653 Zeng, Z., Wang, Z., Gui, K., Yan, X., Gao, M., Luo, M., Geng, H., Liao, T., Li, X.,
654 An, J., Liu, H., He, C., Ning, G., and Yang, Y.: Daily Global Solar Radiation in China
655 Estimated From High-Density Meteorological Observations: A Random Forest Model
656 Framework, 7, e2019EA001058, <https://doi.org/10.1029/2019EA001058>, 2020.
657 Zhou, C., Wang, J., Dai, A., and Thorne, P. W.: A New Approach to Homogenize
658 Global Subdaily Radiosonde Temperature Data from 1958 to 2018, *J Climate*, 34,
659 1163-1183, 10.1175/jcli-d-20-0352.1, 2021.
660 Zhu, C., Wang, B., and Qian, W.: Why do dust storms decrease in northern China
661 concurrently with the recent global warming?, *Geophys Res Lett*, 35,
662 <https://doi.org/10.1029/2008GL034886>, 2008.
663
664

665 Table 1. Trends of Surface Incident Solar Radiation (R_s) in Japan during Specific Time
 666 Periods for Different Types of Datasets^a. Unit: W m⁻² per decade

667

Case ^b	Datasets ^c	1961-1980	1981-1995	1996-2014	1961-2014
Selected 41 Stations	OBS-raw	-12.0**	-2.1	2.4	-0.3
	OBS_HM	-4.8*	-2.1	2.4	1.5**
	OBS_2HM	-0.8*	-2.1	2.4*	0.9**
	SunDu-derived	1.4	-11.3**	1.4	-2.1**
	SunDu-derived_HM	1.4	-1.3*	1.5	0.9**
All Stations	OBS-raw	-11.2**	-1.3	2.2	0.2
	OBS_HM	-8.4**	-1.3	2.2	0.8
	OBS_2HM	0.7	-1.3	2.2	1.6**
	SunDu-derived	2.3*	-10.6**	1.2	-1.9**
	SunDu-derived_HM	1.6	-1.2	1.4	0.9*
Radiative Effect	CCRE series	-1.1	-1.4	-0.0	-1.4**
	Residual series	2.4**	-0.1	1.2*	2.2**

668

669

670

671 ^aThe trend calculations were based on the linear regression method. Values with two
 672 asterisks (**) imply $p < 0.01$, and those with one asterisk (*) imply $0.01 < p < 0.1$.

673 ^b R_s trends were calculated by different numbers of observations, including all stations
 674 that are available on the JMA website and 41 stations (marked with red in Table S1,
 675 detailed in Section 3.1) that are significantly improved after homogenization. This
 676 implies that the sample number has a subtle impact on the trend calculation over Japan.
 677 Radiative effects from clouds and aerosols were also explored.

678 ^cTrend calculations were based on the raw measurements of surface incident solar
 679 radiation (OBS-raw), their homogenized series (OBS_HM), derived incident solar
 680 radiation from sunshine duration hours (SunDu-derived) and their homogenized series
 681 (SunDu-derived_HM). OBS_HM from 1961 to 1970 was further homogenized by
 682 using SunDu-derived_HM as reference data, termed OBS_2HM. It is found that

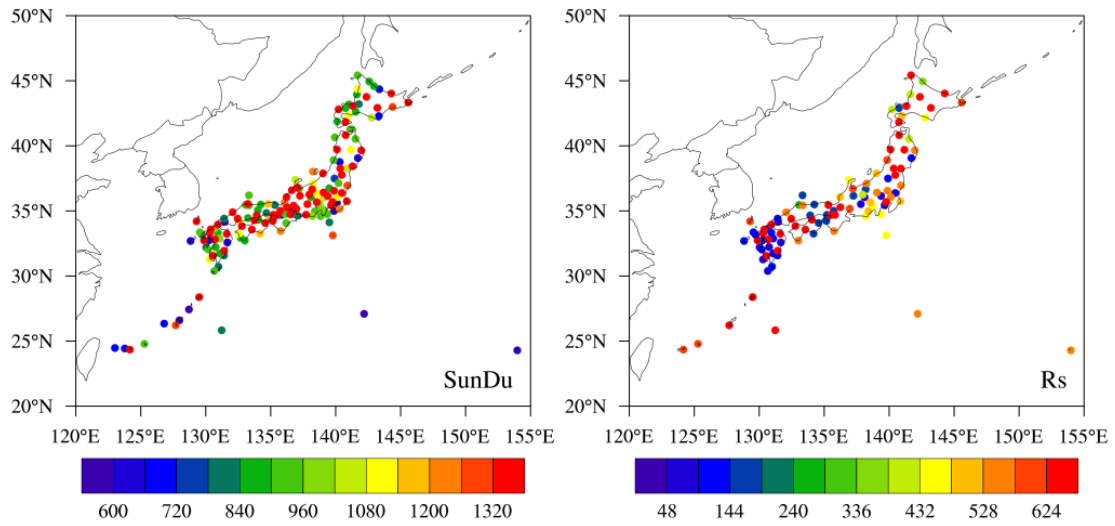
683 homogenized SunDu-derived R_s have the lowest uncertainties among these five
684 datasets in Section 3.1. The cloud cover radiative effect (CCRE) was denoted as the
685 change in R_s produced by a change in cloud cover, and the CCRE calculations were
686 performed following Equation (4) by observed cloud amounts and the cloud radiative
687 effect (CRE) from CERES satellite retrieval. Residual effect series were obtained by
688 removing the CCRE from homogenized SunDu-derived R_s anomalies.
689

690

691 Table 2. Trends of Surface Incident Solar Radiation (R_s) in Japan during Specific Time692 Periods for Different Types of Datasets for All Seasons. Unit: $W m^{-2}$ per decade

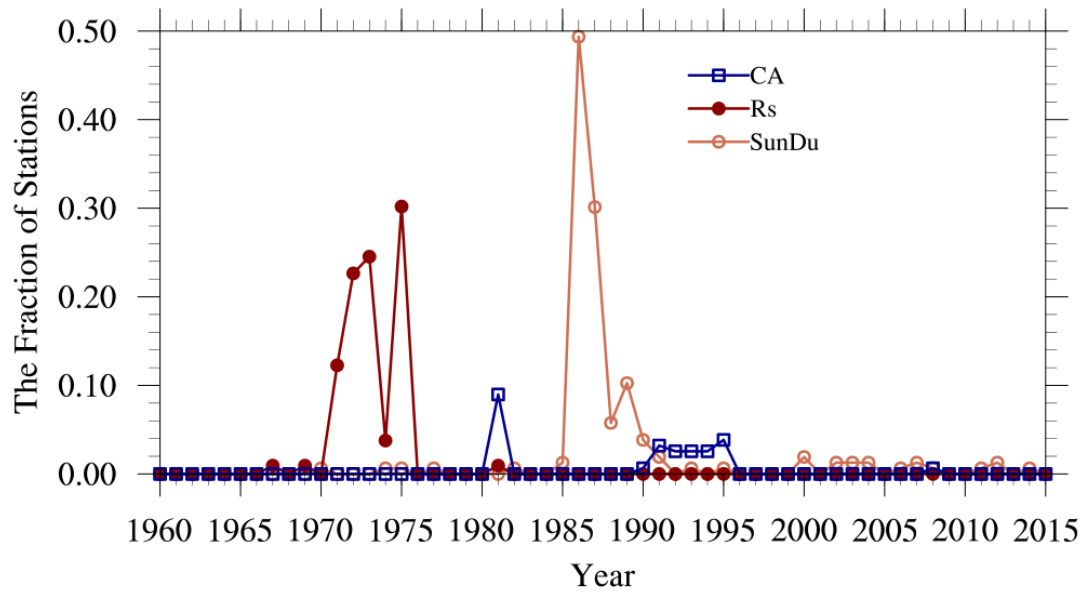
Season	Datasets	1961-1980	1981-1995	1996-2014	1961-2014
Spring	SunDu-derived_HM	3.1	-1.5	3.4*	1.5
	CCRE series	-0.7	-1.6	-1.6	-0.9
	Residual series	4.9**	-0.5**	2.2**	2.8*
Summer	SunDu-derived_HM	1.4	-3.4	0.6	0.4
	CCRE series	-1.9	-2.1	-4.4**	-2.7
	Residual series	2.0**	-1.8	1.5**	2.8
Autumn	SunDu-derived_HM	0.6	1.5	3.3**	1.0*
	CCRE series	-1.3**	1.6	1.6	-0.9
	Residual series	1.8**	0.8**	2.1**	2.0*
Winter	SunDu-derived_HM	0.6	-1.5	-1.6	0.5
	CCRE series	-0.6	-3.3	-0.6	-0.7
	Residual series	1.1**	0.9**	-0.9**	1.2**

693



694

695 Figure 1. The spatial distribution of stations over Japan with observed sunshine duration
 696 (SunDu, 156 stations) and surface incident solar radiation (R_s , 105 stations) data. The
 697 colors indicate the data length of the SunDu records from 1890 to 2015 and R_s records
 698 from 1961 to 2015. Unit: month.

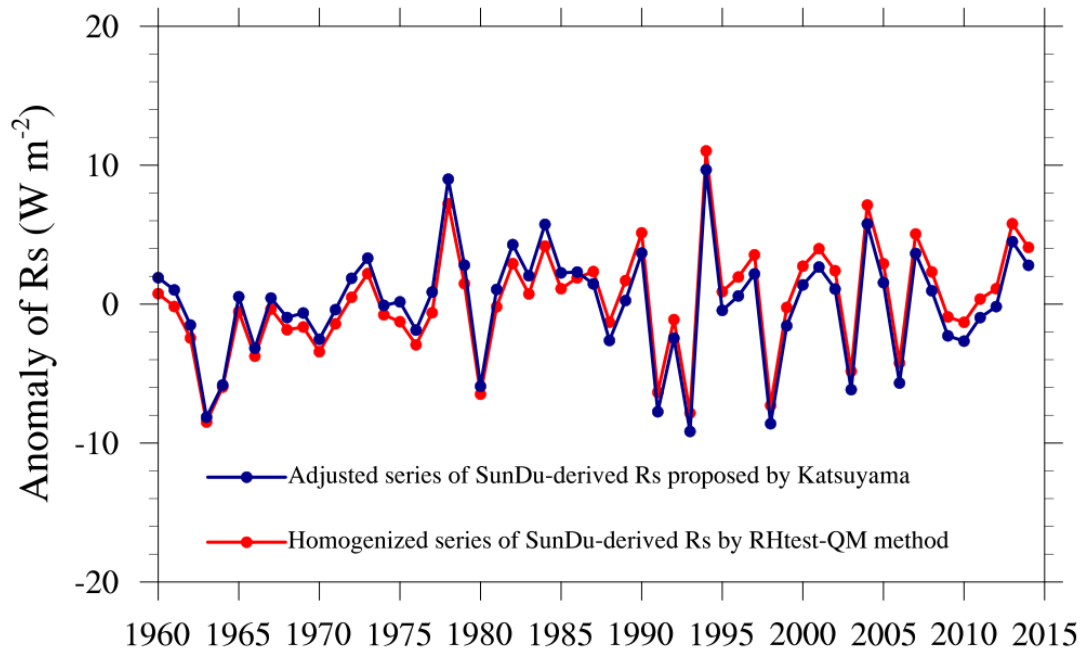


699

700 Figure 2. The fraction of stations that suffer from data inhomogeneity due to site
 701 relocation, change of instruments and measurement method for sunshine duration
 702 (SunDu) records, cloud amount (CA) records and surface incident solar radiation (R_s)
 703 records. In total, there were 156 stations with SunDu records, 105 of which had R_s
 704 records and 155 of which had CA records. The inhomogeneity information shown here
 705 was derived from metadata from
 706 <https://www.data.jma.go.jp/obd/stats/data/en/smp/index.html>, and was used as primary
 707 information to perform the inhomogeneity adjustment in the RHtest method detailed in
 708 Section 2.2.

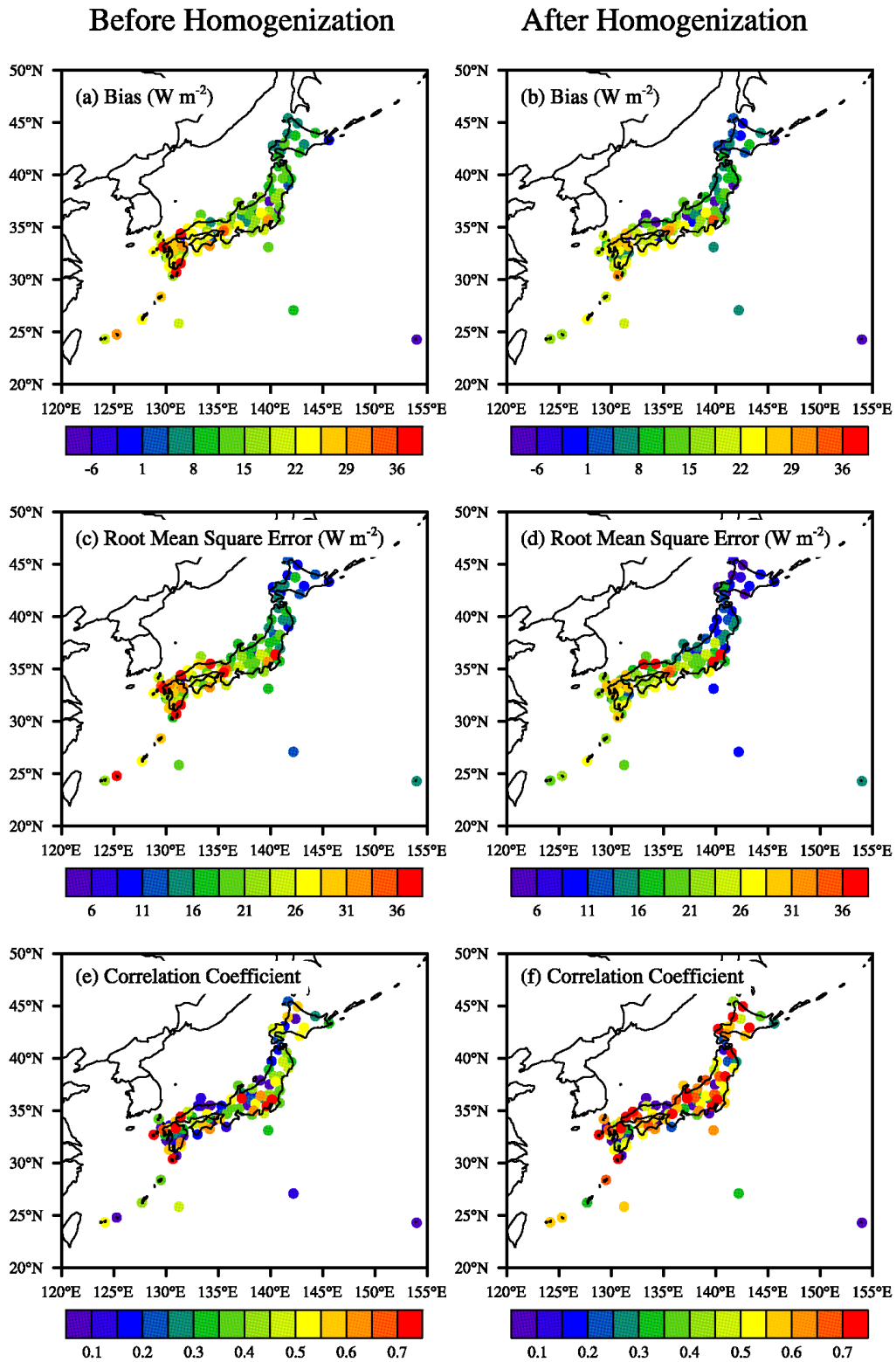
709

710



711

712 Figure 3. The anomalies of surface incident solar radiation (R_s) derived from
 713 homogenized sunshine duration (SunDu) data (red line) by the RHtest-QM method
 714 and other independent data (blue line) adjusted by the method in (Katsuyama, 1987).
 715 Both of the homogenized datasets yield nearly the same R_s variation.

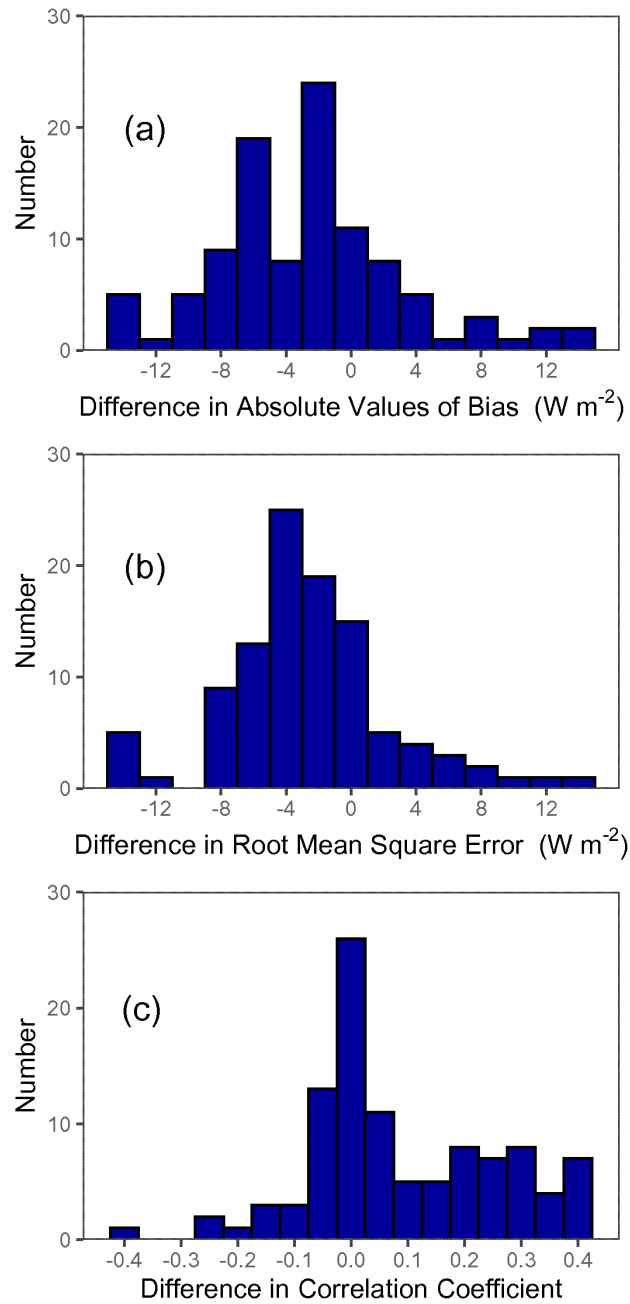


716

717 Figure 4. The spatial distribution of bias, root mean square error and correlation

718 coefficient between SunDu-derived surface incident solar radiation (R_s) and observed

719 R_s before (a, c, e) and after (b, d, f) homogenization. Improvements were made at
720 most sites after homogenization.
721



723

724 Figure 5. Histograms of the difference in absolute values of bias, root mean square

725 error and correlation coefficient between SunDu-derived surface incident solar

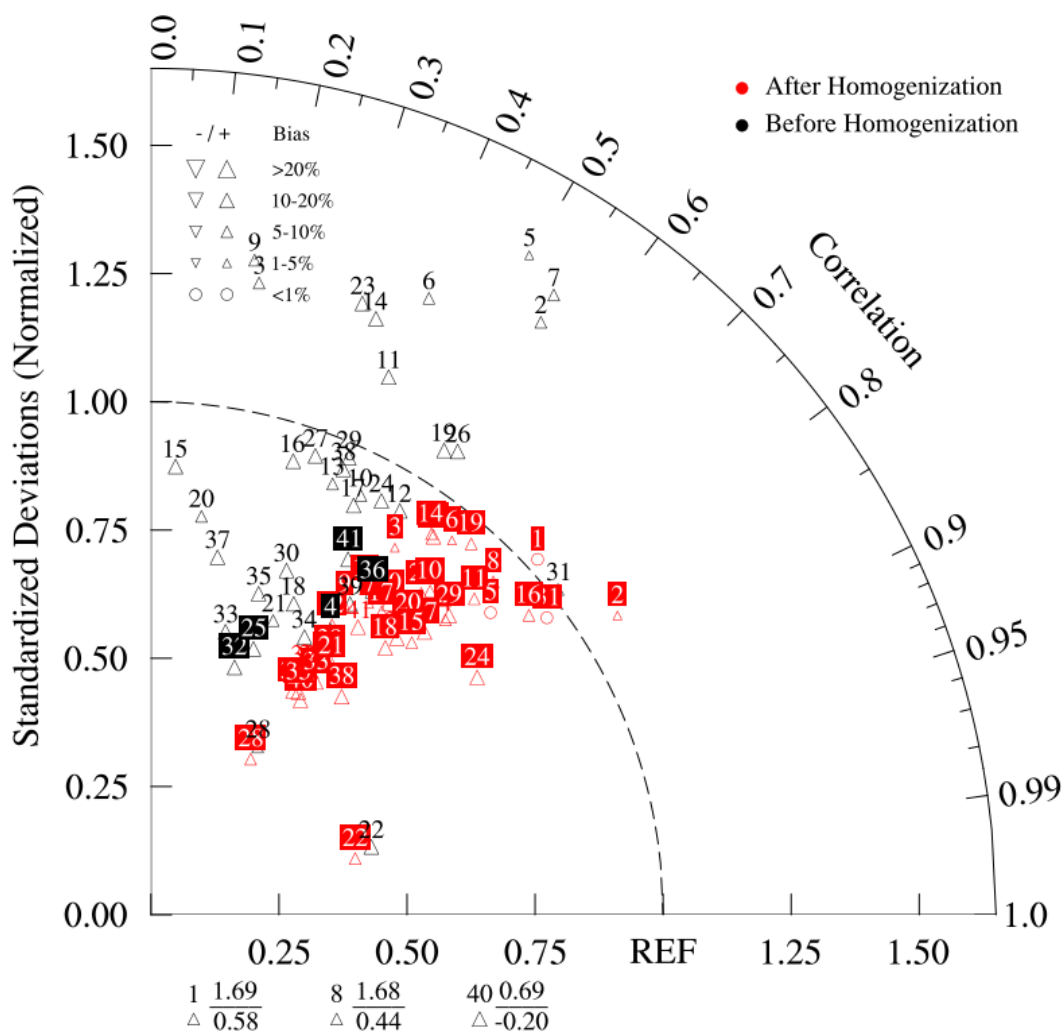
726 radiation (R_s) and observed R_s before and after homogenization. Their differences

727 decrease after homogenization.

728

729

730



731

732

733 Figure 6. Taylor diagram describing the relative biases, standardized deviations and

734 correlation coefficients between the annual observed surface incident shortwave

735 radiation (Rs) and annual sunshine duration (SunDu) derived Rs before and after

736 homogenization at 41 selected stations (Numbered 1-41 here). “REF” can be treated as

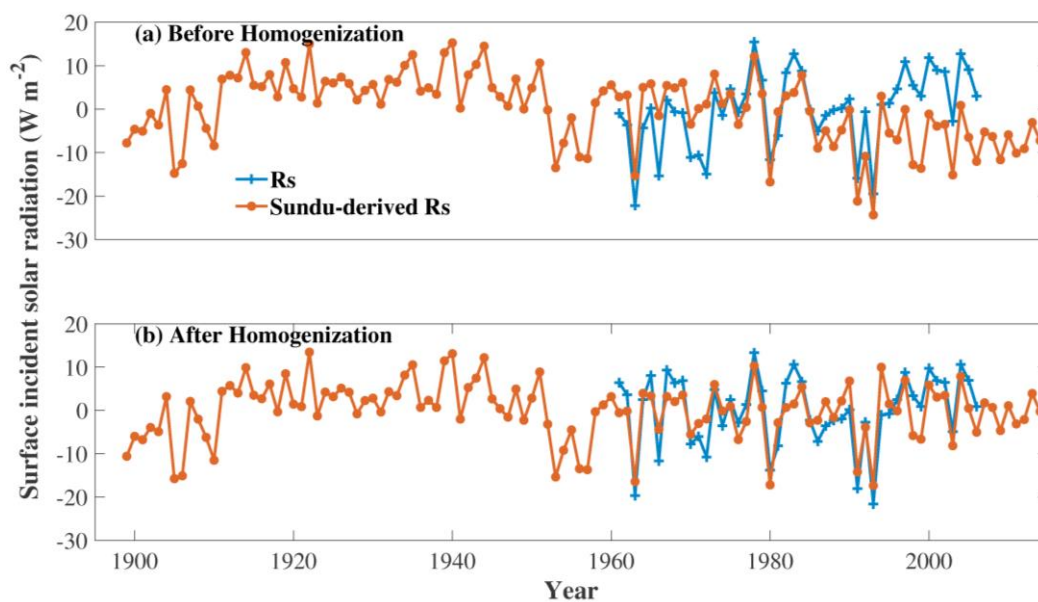
737 the perfect point, where values the closer to this point indicate a better evaluation. The

738 size and direction of the triangles denote the magnitude and negative or positive of
739 biases, respectively. The boxes indicate the smaller bias in Raw (black color) or HM
740 (red color) series. This figure shows that biases decrease at most sites (in red boxes)
741 after homogenization, except for the 5 stations numbered 4, 25, 32, 36 and 41 (in black
742 boxes). Three stations (numbered 1, 8 and 40 in black color) listed below the panel are
743 beyond the scope of the figure, with bias (triangle), ratio of standardized deviation
744 (above the “---” line) and correlation coefficient (below the “---” line) shown. In
745 addition to the improvements in the correlation coefficients after homogenization, the
746 biases and the standard deviations generally become small in this Taylor diagram.

747

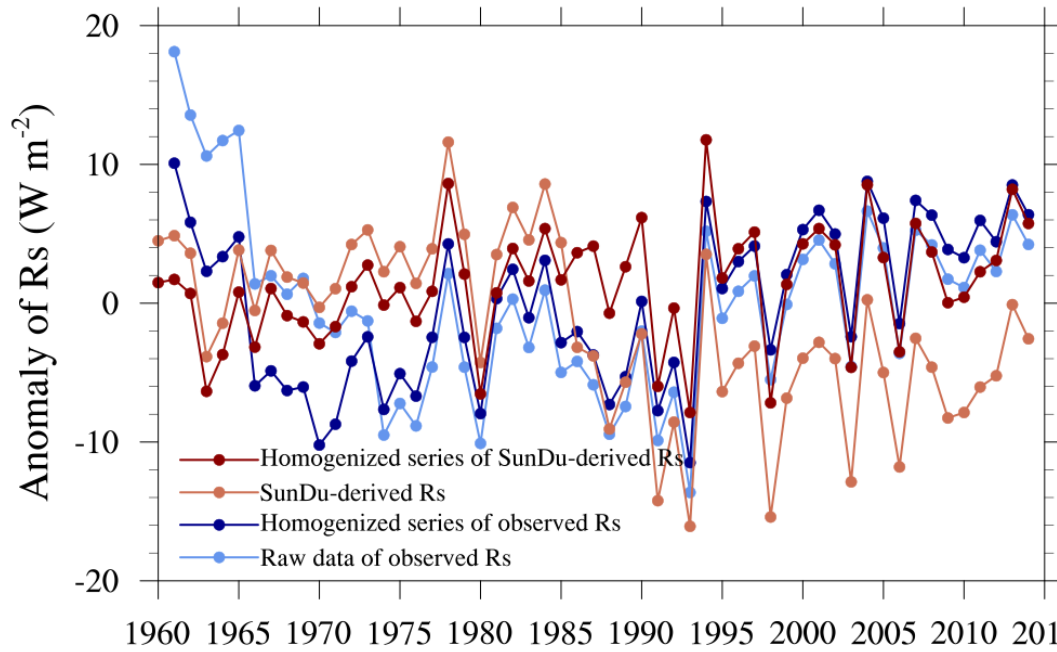
748

749
750
751



752
753
754
755
756
757
758

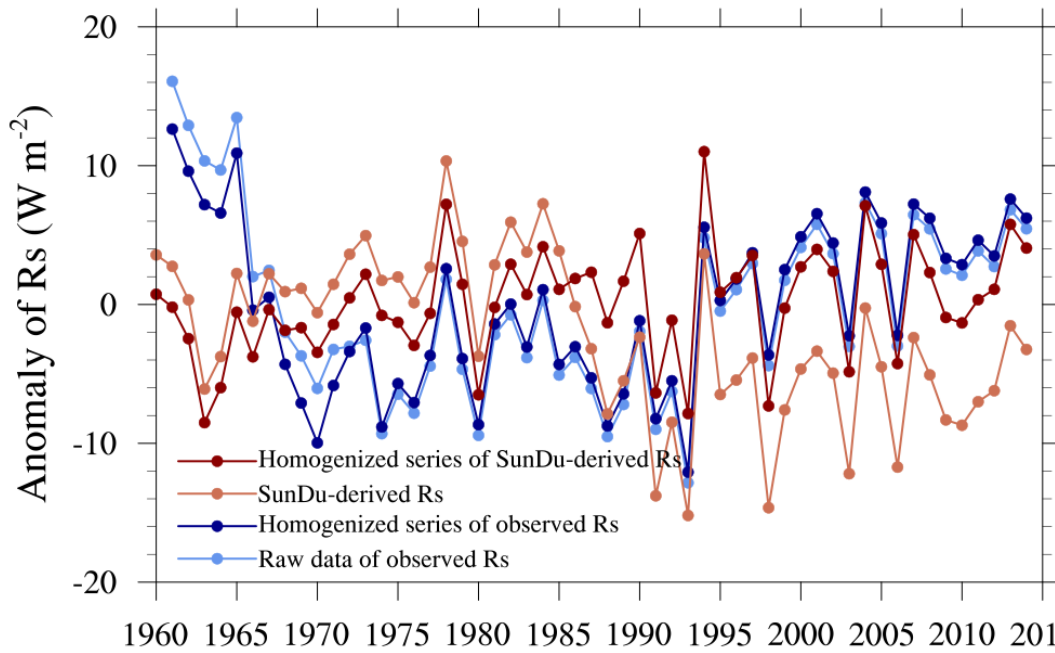
Figure 7. Time series of annual anomalies of observed surface incident solar radiation (R_s) and SunDu-derived R_s at HAMADA site (WMO-ID: 47755, Lat: 34.9° , Lon: 132.07) before and after homogenization.



759

760 Figure 8. Time series of annual anomalies of surface incident solar radiation (R_s) based
 761 on direct R_s observations (light blue line) and their homogenized series (dark blue line)
 762 and sunshine duration (SunDu) derived R_s (light red line) and their homogenized series
 763 (dark red line). All of the lines were calculated based on observations at 41 sites. Details
 764 on how these 41 sites were selected are given in Section 3.1. The R_s variations are nearly
 765 the same as those shown in Figure 7, which were calculated based on all available
 766 observations.

767

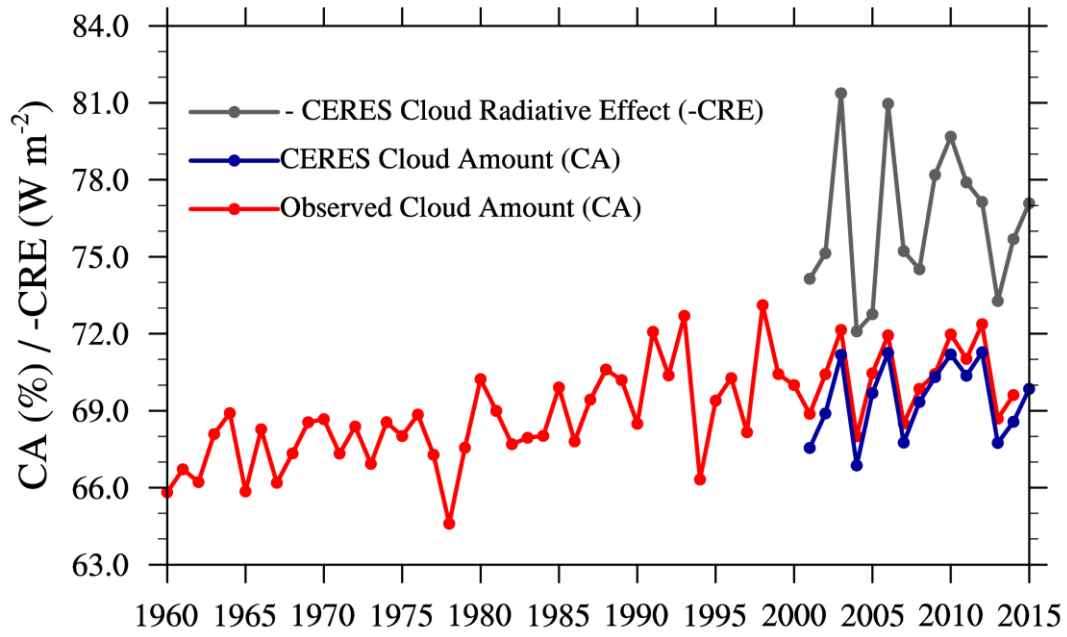


768

769 Figure 9. Time series of annual anomalies of the surface incident solar radiation (R_s)
 770 based on direct observations (light blue line) and their homogenized series (dark blue
 771 line) and sunshine duration (SunDu) derived R_s (light red line) and their homogenized
 772 series (dark red line). All of the lines were calculated based on as many observations as
 773 possible. The light blue line and dark blue line were calculated from the R_s observations
 774 at 105 sites, while the light red line and dark red line were derived from the SunDu-
 775 derived R_s at 156 sites. The R_s variations are nearly the same as those shown in Figure
 776 6, which were calculated based on the 41 selected sites in Section 3.1. Large
 777 discrepancies were found in the homogenized data series (dark blue and dark red lines).

778

779



780

781 Figure 10. The cloud amount (CA) from CERES (blue line) agrees well with that
 782 derived from surface observations (red line) over Japan. At the annual time scale, the
 783 negative cloud radiative effect (-CRE, grey line) in CERES correlated well with the
 784 cloud amount.

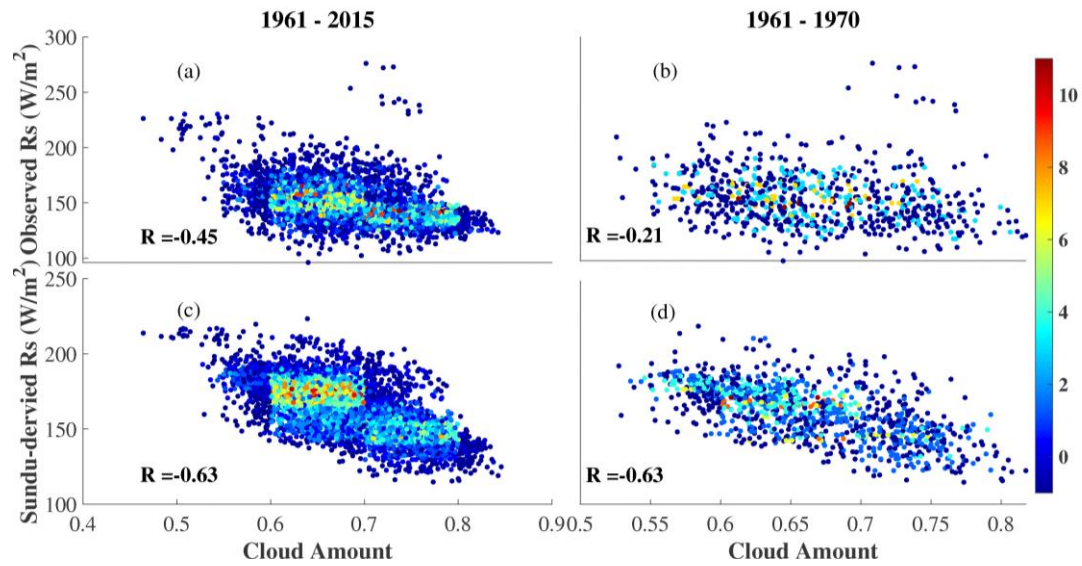
785

786

787

788

789



790

791 Figure 11. Scatter plot of homogenized monthly surface incident solar radiation (R_s)

792 (observed and SunDu-derived solar radiation) as a function of ground-based

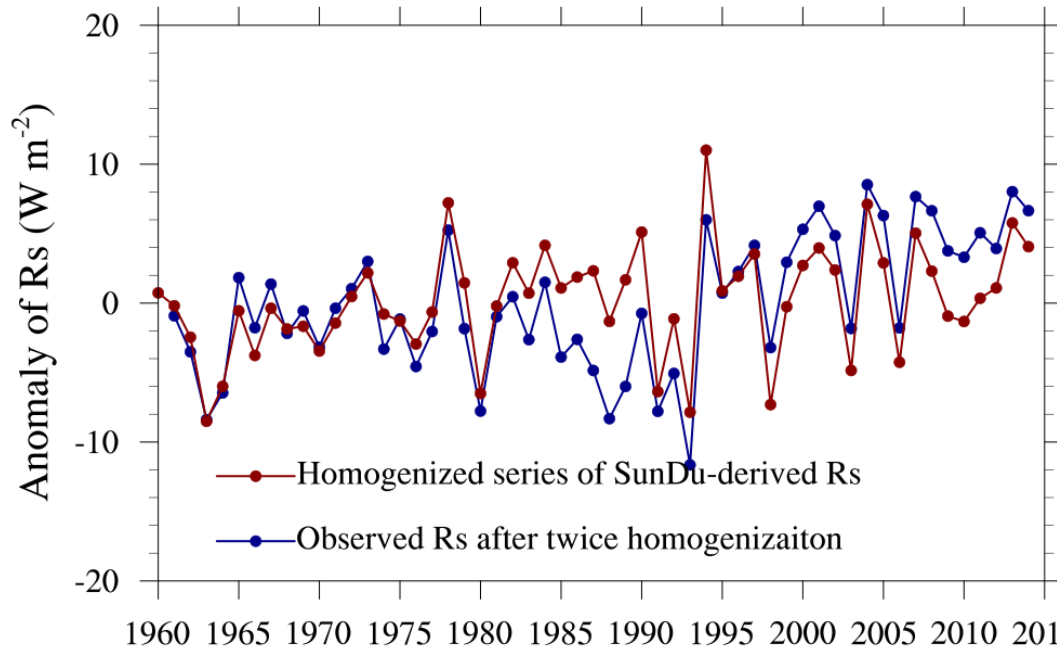
793 observations of cloud amount over Japan at all stations only when both cloud amount

794 data and observed R_s data are available. (a) and (c) for 1961-2015, (b) and (d) for

795 1961-1970. The smallest correlation coefficient in (b) indicates that the observed R_s

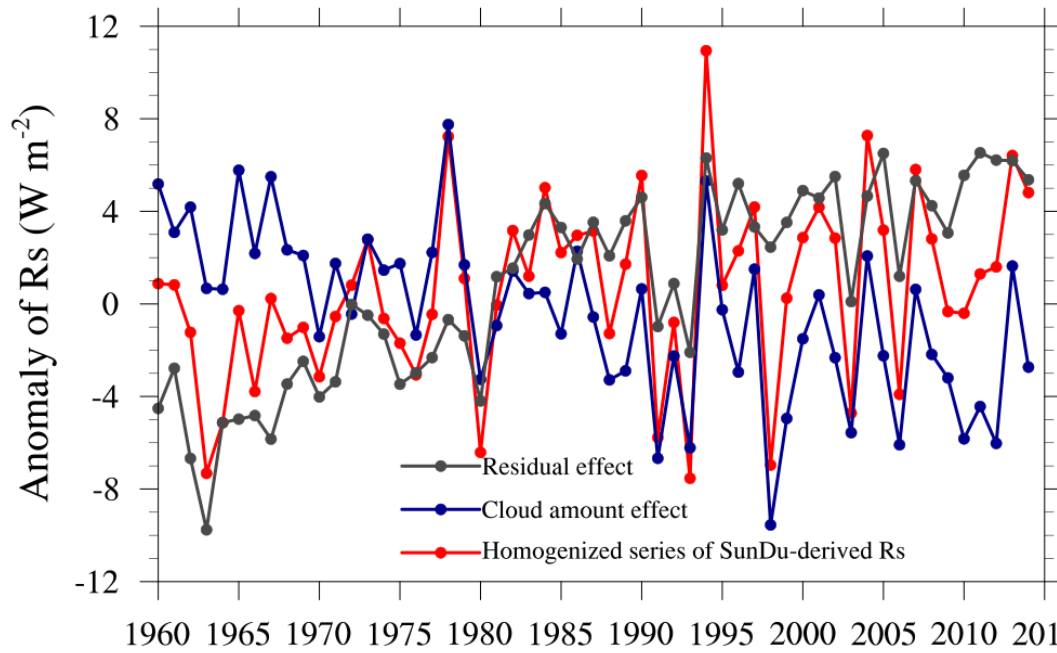
796 data are spurious for 1961-1970, and SunDu-derived R_s are more convincing.

797



798

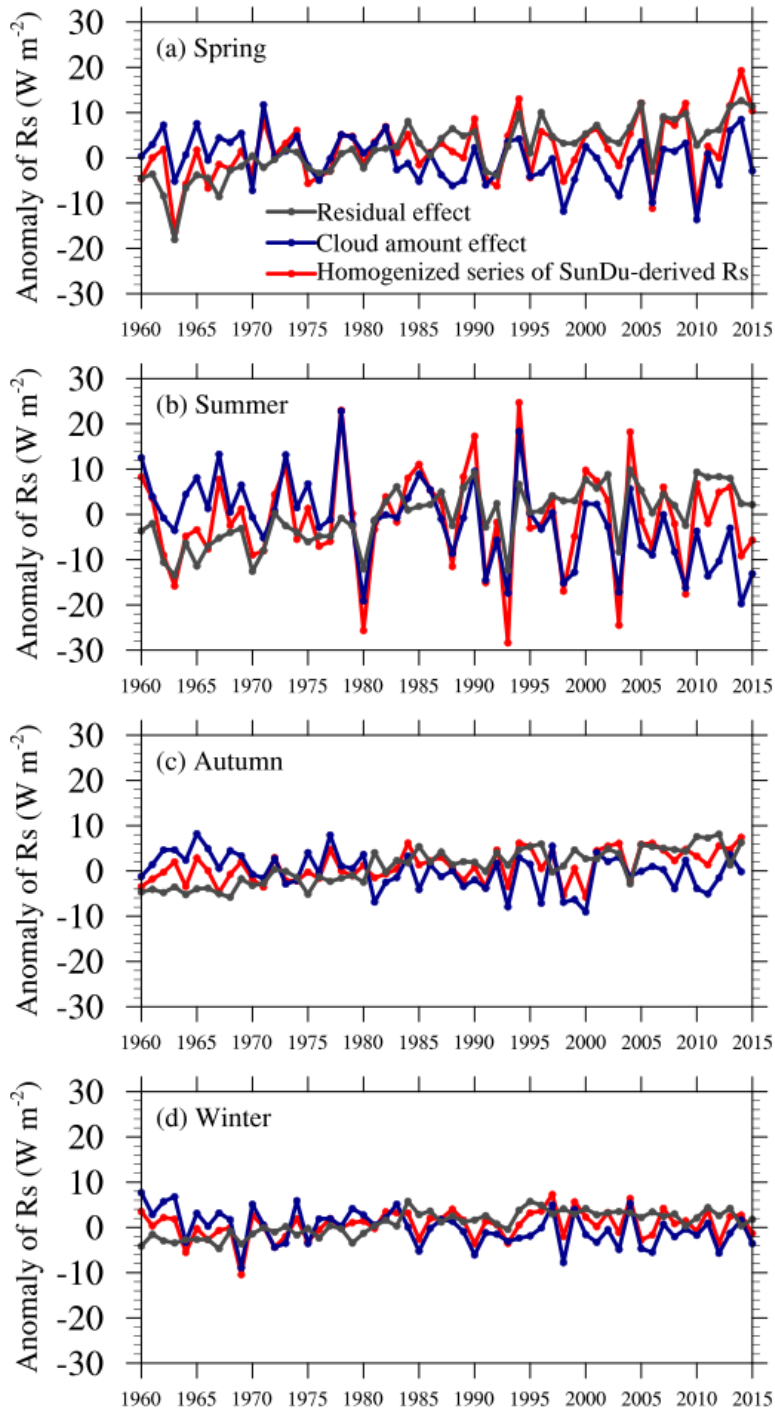
799 Figure 12. Time series of annual anomalies of the surface incident solar radiation (R_s)
 800 based on R_s observations after two homogenizations (dark blue line). The homogenized
 801 series of observed R_s from 1961 to 1970 shown in Figure 7 was tuned by RHtest method
 802 again using the homogenized series of SunDu-derived R_s (dark red line in Figure 7 and
 803 Figure 10) as a reference.



804

805 Figure 13. Area-averaged anomalies of homogenized SunDu-derived R_s (red line) over
 806 Japan. The cloud cover radiative effect (CCRE, blue line) was denoted as the change in
 807 R_s produced by a change in cloud cover and calculated following Equation (4) by
 808 observed cloud amounts and cloud radiative effect (CRE) from the CERES satellite
 809 retrieval. The residual effect (grey line) was obtained by removing the cloud cover
 810 radiative effect (CCRE) from the homogenized SunDu-derived R_s anomalies.

811



812

813 Figure 14. Same as Figure 12 but for the four seasons. The decrease in Asian spring

814 dust may have triggered the brightening over Japan for 1961-2015, as the R_s in spring

815 increases most among the seasons.